J Electroceram (2006) 16: 127–133
DOI 10.1007/s10832-006-4300-5

Size-controllable barium titanate nanopowder synthesized via one-pot solvothermal route in a mixed solvent

Bo Hou · Zhijie Li · Yao Xu · Dong Wu · Yuhan Sun

Received: 30 October 2004 / Revised: 8 July 2005 / Accepted: 17 August 2005

Abstract Barium titanate nanopowder was synthesized via solvothermal route using water-ethanol-ethylene glycol monomethyl ether as mixed solvent and $TiCl_4$-$Ba(OH)_2 \cdot 8H_2O$ as precursors. The effects of water amount in a mixed solvent, synthetic temperature and reaction time on microstructure and particle size of the as-prepared barium titanate powder were investigated systematically. The results show that the particle size of barium titanate powder could be tuned by varying the synthetic parameters. The procedure presented here provides a simple route to the preparation of barium titanate nanopowder with controllable particle size.

Keywords Barium titanate · Solvothermal · Nanopowder

1. Introduction

Barium titanate ($BaTiO_3$) is one of the most widely used and studied ferroelectric materials in the electro-ceramics industry because of its remarkable properties such as high dielectric constants, excellent ferroelectric properties, and large electro-optic and non-linear optic coefficients. Conventional processes (for example, solid-state synthesis [1–3] and co-precipitation [4, 5]) often give rise to $BaTiO_3$ powder in the range of micrometer due to high temperature calcinations, and cannot satisfy the growing demands for miniaturization of electronic device and downsizing of electronic components. Thus, other chemical methods capable of producing ultrafine $BaTiO_3$ powder, such as sol-gel method [6, 7], hydrothermal (solvothermal) method [8–12], sol-precipitation process [13], low temperature direct synthesis method [14], have become currently an active area of research. Of these wet chemical methods, hydrothermal (solvothermal) method possesses several advantages involving the production of fine uniform particles with a narrow size distribution and the ability of preparation of crystalline $BaTiO_3$ without high-temperature calcinations.

There were many studies about hydrothermal synthesis of $BaTiO_3$, but only a few literatures reported on the preparation of $BaTiO_3$ via a solvothermal process using non-aqueous solvent as reaction media. J.F. Bocquet et al. [15] showed that the $BaTiO_3$ powder with average size of 12 nm could be synthesized using alkoxide $BaTi(O\text{-}iC_3H_7)_6$ as precursors and isopropanol as solvent under high pressure, and that the particle size depended on the reaction conditions. Moreover, they used a set of complicated equipment to control reaction pressure. P. Pinceloup et al. [16] revealed that increasing isopropanol amounts in the reaction media could increase the rate of nucleation and then decrease the size of particles. B.K. Kim et al. [17] glycothermally synthesized $BaTiO_3$ using $Ba(OH)_2 \cdot 8H_2O$ and titanium isopropoxide as precursors and 1,4-butanediol as solvent under autogeneous vapor pressures. They found that glycolic solution acted as a strong oxidizer instead of the highly alkaline conditions in the hydrothermal reaction. These studies revealed that the size and shape of $BaTiO_3$ prepared via solvothermal reaction could be controlled by adjusting processing parameters. Although all these methods can attain ultrafine $BaTiO_3$ powder with narrow particle size distribution, the expensive reactant or special equipments used make them unsuitable to prepare $BaTiO_3$ in large scale. Many papers have investigated the

B. Hou · Z. Li · Y. Xu · D. Wu · Y. Sun (✉)
State Key Laboratory of Coal Conversion, Institute of Coal Chemistry, Chinese Academy of Sciences, Taiyuan, 030001, China
email: yhsun@sxicc.ac.cn

B. Hou · Z. Li
Graduate School of the Chinese Academy of Sciences, Beijing, 100039, China

Table 1 The data of reaction conditions

	Content of solvent in reaction media (mL)			Reaction conditions	
Sample	Water	Ethanol	$HO(CH_2)OCH_3$	T (°C)	Time (h)
S-1	80	–	–	140	48
S-2	60	10	10	140	48
S-3	40	20	20	140	48
S-4	20	30	30	140	48
S-5	–	40	40	140	48
S-6	40	20	20	140	168
S-7	40	20	20	200	48

effects of different precursors and solvents on the properties of $BaTiO_3$. Most literatures about solvothermal $BaTiO_3$ did not investigate the dissolvability of $Ba(OH)_2 \cdot 8H_2O$ in nonaqueous solvent. In addition, among these, although newly-prepared amorphous TiO_2 or $Ti(OH)_4$ gel having the best active reactivity of all Ti-precursors for the production of $BaTiO_3$ nanopowder via solvothermal (hydrothermal) method had already been testified by many researchers [9, 16, 17], it brought about more experimental steps to result in high industry cost.

In this paper, a solvothermal method for the synthesis of $BaTiO_3$ using low-cost reactant $TiCl_4$ as raw material in a mixed solvent was reported. This method provides a simple one-pot solvothermal route to the preparation of the size-controllable $BaTiO_3$ nanopowder.

2. Materials and methods

2.1. Materials

All materials were used as received, including titanium tetrachloride ($TiCl_4$, 99%), absolute ethanol (CH_3CH_2OH, 99.7%), ethylene glycol monomethyl ether ($HO(CH_2)OCH_3$, 100%), barium hydroxide ($Ba(OH)_2 \cdot 8H_2O$, 98%) and sodium hydroxide (NaOH, 96%).

2.2. Preparation of $BaTiO_3$

A typical experiment procedure was as follows: 1 mL of $TiCl_4$ was added dropwise into 20 mL of absolute ethanol to form a clear yellowish solution A at room temperature. On the other hand, 3.44 g of $Ba(OH)_2 \cdot 8H_2O$ (Ba/Ti mol ratio is 1.2) was dissolved into 20 mL of $HO(CH_2)OCH_3$ to form solution B. The solution A was added dropwise into the solution B (a white stiff suspension appeared), followed by stirred for 10 min, then 40 mL of distilled water (the total volume of the mixed solvent is 80 mL) was dropped into the above mixture (the white slurry became clear rapidly). After the addition of 5 g of NaOH into the obtained mixture (a white suspension appeared again), the final mixture was heated in a 100 mL autoclave at 140°C for 48 h. After the reaction was completed, the gained precipitation was filtrated and washed with distilled water, then dried in oven at 110°C for 12 h. In order to get a comparison, a sample was prepared using pure water as the solvent via the above-mentioned procedure.

To investigate the effects of synthetic parameters on the properties of $BaTiO_3$, the reaction temperature, the reaction time and the ratio of $H_2O/CH_3CH_2OH/HO(CH_2)OCH_3$ were varied. The designations of the corresponding samples and their preparation conditions were showed in Table 1 in detail.

2.3. Characterization

X-ray diffraction patterns (XRD) were recorded on a D/max2500 powder diffractometry system with CuKα-radiation (40 kV, 20 mA) using a 0.05° step size at the range of $20° < 2\theta < 60°$ and a 0.01° step size at the range of $43° < 2\theta < 47°$, respectively. The Gauss peak fit model was used in the XRD analysis. The crystallite size of $BaTiO_3$ was estimated from the (200) diffraction peak using the Scherrer equation [18]:

$$d_{XRD} = 0.94\lambda/\beta \cos\theta$$

where λ (0.15406 nm) is the characteristic wavelength, β is the full-width at half-maximum (FWHM) and θ is half the diffraction angle of the centroid of the peak. The morphology of the samples was observed on a transmission electron microscopy (TEM) (Hitachi-600–2, Japan, 75 kV). Samples were scattered by ultrasonics for 10 min in ethanol, and two drops were taken onto carbon-coated copper grids. The BET surface areas of the samples were measured on a Micromeritics Tristar 3000 sorptometer. Prior to the measurement, all samples were outgassed at 120°C and 10^{-6} mmHg overnight. The particle size of the samples was estimated using the equation [19]:

$$d_{BET} = 6/\rho S_W$$

where ρ (6.08 g/cm^3) is the standard density of $BaTiO_3$ and S_W is the BET surface area of the sample. Raman

spectroscopy was carried out on microscopic confocal Raman spectrometer (RM2000, Britain) using a 100 mW Ar laser with a wavelength of 514.5 nm. Spectra were measured over the range 60–1100 cm^{-1}.

3. Results and discussion

X-ray diffraction patterns of the samples S-1, S-2, S-3, S-4 and S-5 are shown in Fig. 1. No splitting for (002)/(200) ($2\theta \approx 45^{\circ}$) peak was observed for these samples, implying that the samples are perovskite-type cubic $BaTiO_3$ [14]. There are no other impurities existing except for orthorhombic $BaCO_3$ (JCPDS No. 5-378) as a by-product, which is labeled with asterisk mark in Fig. 1. Under otherwise the same reaction conditions, the decrease of the water amount in solvent led to the decreased crystallinity of products and the decreased amount of $BaCO_3$, suggesting that water in solvent is in favor of the formation of $BaTiO_3$.

Fig. 2 exhibits (200) planes of the samples S-1, S-2, S-3, S-4 and S-5 measured with a step of 0.01°. On the assumption that the crystal structure of $BaTiO_3$ prepared is cubic symmetry Pm3 m, lattice constants *a*-axis is estimated from *d-value* of XRD patterns of $BaTiO_3$ and the crystal size is also estimated by Scherrer equation [18, 20]. The (200) peak of the samples shifted toward lower angles with decreasing the water amount in solvent from 75% to 0% (see Fig. 2). At the same time, the lattice constant *a-value* estimated from *d-value* of XRD patterns increased from 0.4016 to 0.4047 nm and the crystal size of $BaTiO_3$ decreased from 21.5 to 8.0 nm. It is well known that many factors, such as defects and impurities in the grain lattice of powders, can affect the lattice parameter of the powder [21]. The defects and impurities mainly result from synthesis method and reagents used in the experiment. A decrease in the scattering angles indicates an overall increase in lattice constants and an expansion of the unit cells [22]. The hydroxyl group can often exist in the lattice of $BaTiO_3$, when the $BaTiO_3$ powder

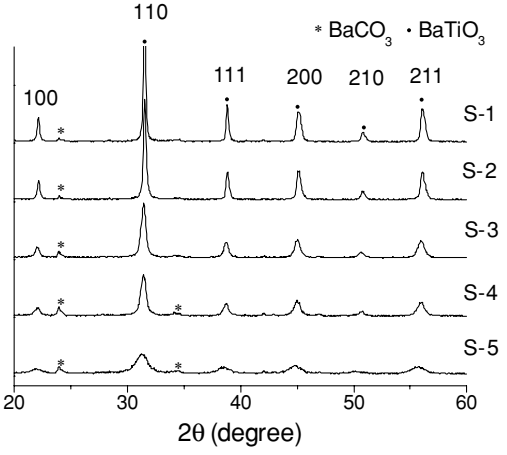

Fig. 1 XRD patterns of the samples S-1, S-2, S-3, S-4 and S-5

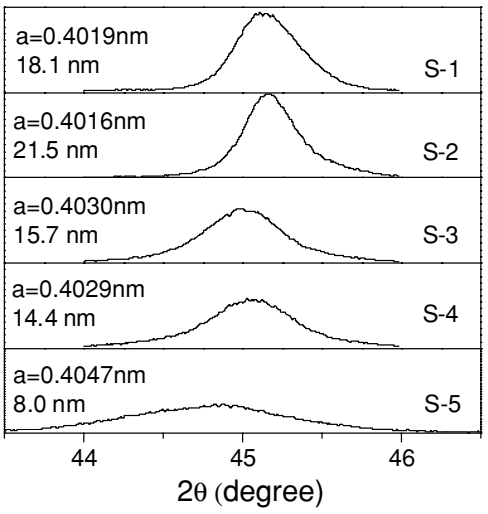

Fig. 2 Water amount dependence of the (200) peak in X-ray diffraction patterns of the samples S-1, S-2, S-3, S-4 and S-5

is synthesized in aqueous media, for example, hydrothermal and co-precipitation procedure [23]. The lattice cell of the $BaTiO_3$ expands because there is water in reaction system and interstitial hydrogen ion may exist in $BaTiO_3$ lattice. The increase of lattice constants *a-value* means that the amount of lattice hydroxyl group increases with decreasing the water amount in solvent [24] and that the contamination by hydroxyl group into a $BaTiO_3$ unit cell mainly result from the non-aqueous solvent in our experiment. This can be confirmed that the largest lattice constants *a-value* is attained in the solution without adding water. The results show that the non-aqueous solvent in reaction media play an important role on the microstructure of $BaTiO_3$ synthesized via solvothermal method.

Raman spectra of the samples S-1, S-2, S-3, S-4 and S-5 are shown in Fig. 3. The peaks around 720, 515, 305 and 268

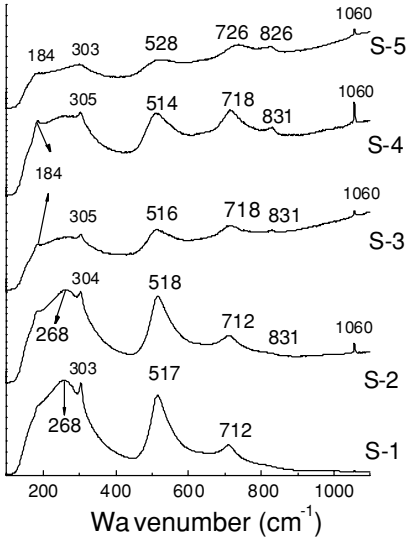

Fig. 3 Raman spectra of the samples S-1, S-2, S-3, S-4 and S-5

cm^{-1} are assigned to the overlap of E(4LO) + A1(3LO), E(4TO) + A1(3TO), E(3TO) + E(2LO)+B1 and A1(2TO), respectively [25, 26]. But the only peak around 305 cm^{-1} was looked upon as the characteristic of Raman-active modes resulting from the tetragonal phase for the as-prepared $BaTiO_3$ nanocrystals [11, 27]. The results suggest that the as-prepared $BaTiO_3$ nanopowder is at least tetragonal in the local range [11] or cubic phase with some tetragonality that cannot be detected with XRD measurement. With decreasing the water amount in solvent, the 305 cm^{-1} peak weakened, suggesting that the water amount in solvent is in favor of the formation of tetragonal phase. The peak around 830 cm^{-1} appeared with increasing concentration of the lattice hydroxyl group. Thus, we assigned this peak to deformation vibration of the lattice hydroxyl group. At the same time, the 268 cm^{-1} peak also obviously weakened with decreasing the water amount in solvent, suggesting that it is also strongly dependent on the concentration of the lattice hydroxyl group. There are no peaks of Ti-containing precursors, which mean that the reaction is complete. It should be noted that all spectra contain a weak peak at 1060 cm^{-1} associated with a small amount of $BaCO_3$ resulted from reaction of $Ba(OH)_2$ and CO_2 in air. The amount of $BaCO_3$ can be reduced by carrying out the reaction in inert atmosphere or washing the product using mild acid solution instead of distilled water.

There are three routine methods to measure the particle size, i.e., BET, XRD and TEM. The XRD measurement determines the crystal size of the as-prepared $BaTiO_3$ [20], TEM provides an image of particles that may be single crystal or crystal aggregates and the BET method determines the aggregate size or shows whether the particle shape of the as-prepared powder can be taken as perfectly spherical or not [19]. The results of the BET surface area, particle size estimated from the BET surface area and crystal size estimated from XRD of the samples S-1, S-2, S-3, S-4 and S-5 are shown in Table 2. It can be seen that with decreasing the water amount in solvent, there was a significant increase of the BET surface area, i.e., a decrease of particle size. The largest BET surface area (109.22 m^2/g) and the smallest crystal size (8.0 nm) was obtained for S-5 prepared in nonaqueous solvent at 140°C for 48 h. It was noticed that the crystal size of the sample obtained from the Scherrer equation was smaller than that estimated from the BET surface area. When the sample was prepared in pure water media, the particle size estimated from BET surface area was far larger than the crystal size from XRD, suggesting the as-prepared particle using pure water as solvent is built up of more small grains. Fig. 4 showed the relations between the water amount in solvent and *a-value*, crystal size estimated from XRD and particle size estimated from the measured BET surface areas of powder. From Fig. 2 and Fig. 4, when the sample was synthesized using pure water as solvent, its crystal size, lattice constants *a*-axis and the location of (200) peak did not follow the change trends of that prepared at the condition of mixed solvent, possibly because the formation mechanism of $BaTiO_3$ was not completely uniform due to different reaction process in pure water from that in mixed solvent or non-aqueous solvent.

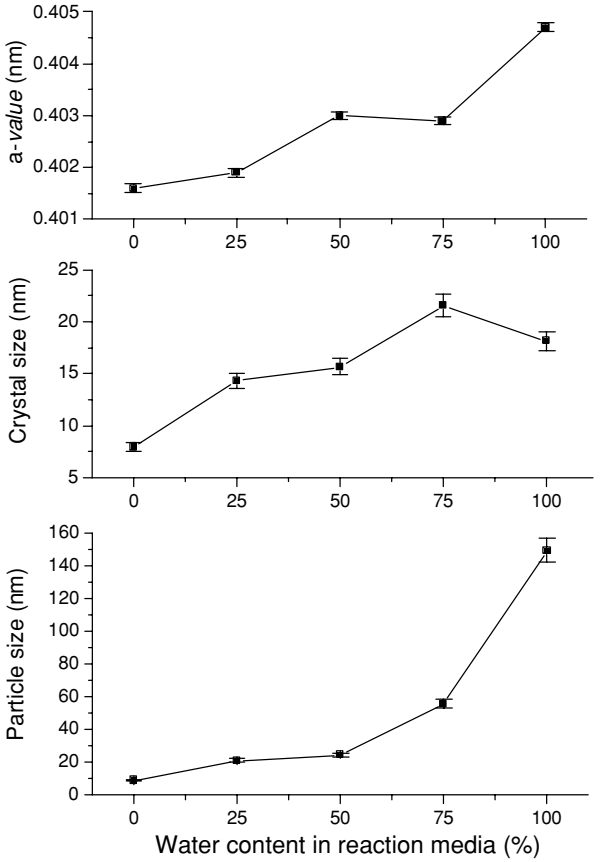

Fig. 4 *a-value*, crystal size and particle size estimated from the measured BET surface areas of powder dependence of water amount in reaction media. (S-1: 100%; S-2: 75%; S-3: 50%; S-4: 25%; S-5: 0%)

Table 2 The lattice constants *a-value*, BET surface area, crystal size attained from XRD and particle size attained from BET

Sample	Water amount in solution (vol%)	Lattice constants *a-axis* (nm)	BET surface areas (m^2/g)	Crystal size (nm)	Particle size (nm)
S-1	100	0.4019	6.61	18.1	149.3
S-2	75	0.4016	17.68	21.5	55.8
S-3	50	0.4030	40.35	15.7	24.5
S-4	25	0.4029	46.98	14.4	21.0
S-5	0	0.4047	109.22	8.0	9.0

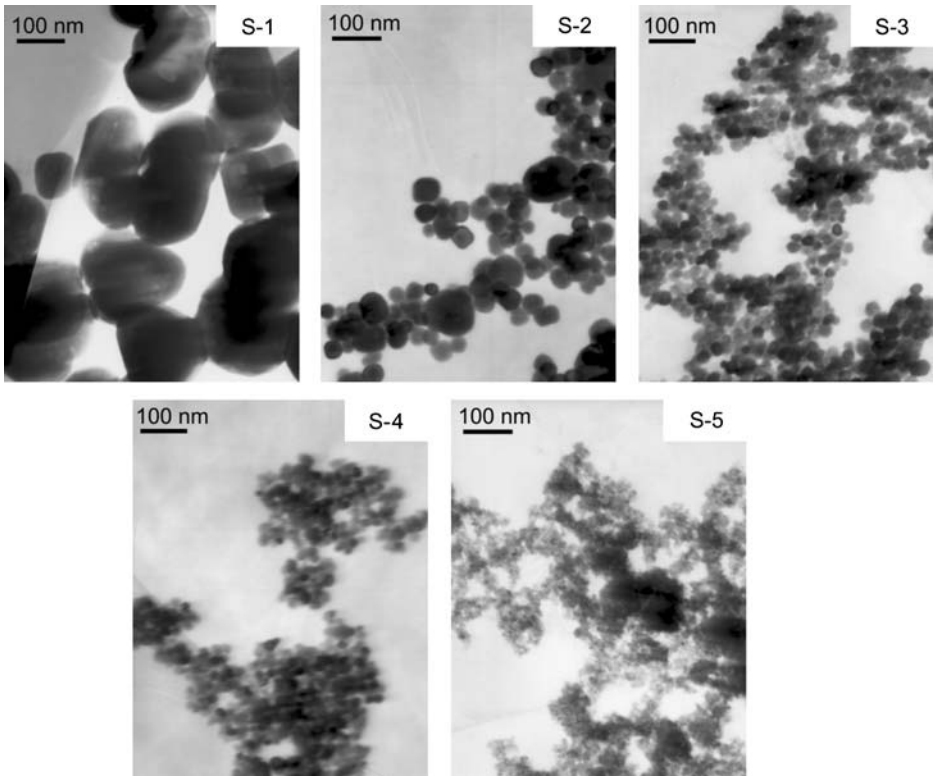

Fig. 5 TEM images of the samples S-1, S-2, S-3, S-4 and S-5

Fig. 5 shows TEM images of the samples S-1, S-2, S-3, S-4 and S-5. It is clearly observed that the particles prepared in the mixed solvent are smaller and more uniform than that prepared in pure water solvent. When the synthesis was performed in the mixed solvent, the particle size drastically decreased with decreasing the water amount in solvent. It is consistent with that attained from BET and XRD. Although the crystal size of $BaTiO_3$ powders prepared from pure water was only 18.1 nm (deduced from XRD), its particle size estimated from TEM is more than 100 nm. The particle size of the samples synthesized in mixed solvent or non-aqueous solvent is very close to the crystal size, suggesting that the mixed solvent may obviously retard the particle growth after nucleation by aggregation.

TEM images and XRD patterns of the samples S-6 and S-7 are shown in Figs. 6 and 7 Comparing with the sample S-3, the average particle size of S-6 and S-7 increased to 20 nm and 80 nm. This means that both extended time and elevated temperature result in bigger particle and that the particle growth of sample prepared at elevated temperature is more obvious than that at extended time. Raman spectra of the samples S-6 and S-7 are shown in Fig. 8. A distinct peak around 305 cm^{-1} (see Fig. 8b) was observed for S-7, but not S-6 and S-3. This indicates that elevated temperature is in favor of not only growing up of $BaTiO_3$ particle but also formation of tetragonal phase [11]. Although larger $BaTiO_3$ particle can be attained for extended time, there is no distinct change around 305 cm^{-1} peak, suggesting that reaction time has no marked influence on the formation of tetragonal phase.

Fig. 9 exhibits XRD patterns of (200) planes of the samples S-6 and S-7 measured with a step of 0.01°. At the same reaction temperature, the diffraction angle of (200) planes, *a-value* and crystal size of $BaTiO_3$ are almost constant. When the reaction was carried though at higher temperature, the diffraction angle shifted from 44.8° to 45.1°, *a-value* decreased from 0.4047 nm to 0.4030 nm and the crystal size increased from 8.0 nm to 21.9 nm. Although the reaction temperature and time have notable effect on the particle size, the reaction time has no obvious effect on crystal parameters of $BaTiO_3$ synthesized with nonaqueous solvent.

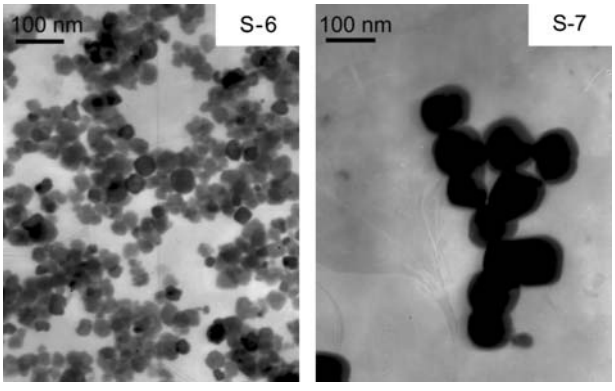

Fig. 6 TEM images of the samples S-6 and S-7

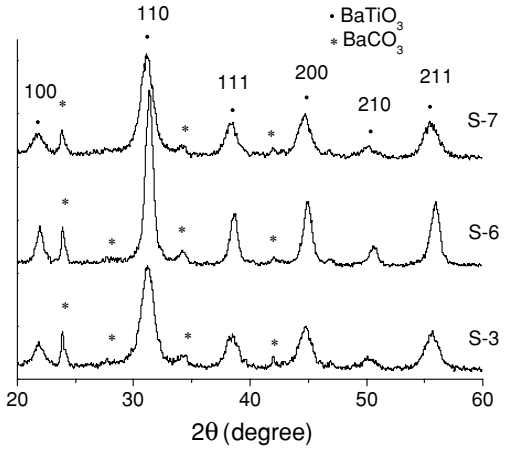

Fig. 7 XRD patterns of the samples S-6 and S-7 as compared with S-3

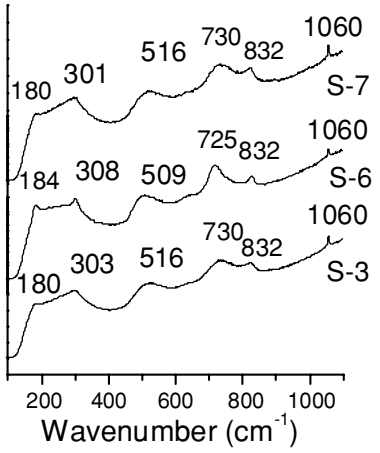

Fig. 8 Raman spectra of the samples S-6 and S-7 as compared with S-3

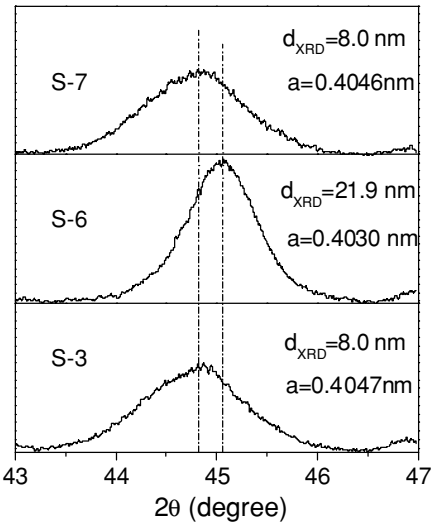

Fig. 9 A (200) plane of the samples S-6 and S-7 as compared with S-3

The mechanism of nucleation and growth of $BaTiO_3$ particle prepared under our experimental conditions is followed by dissolution-precipitation mechanism and aggregative method. It can be easily observed in Fig. 5 and Fig. 6 that the particle size of $BaTiO_3$ was strongly dependent on solvent ratio, reaction temperature and time. With decreasing the water amount in solvent, the polarity of solution decreases and the solubility of reactant decreases, therefore the rate of nucleation increases, which leads to a much greater number of particles [16]. After nucleation, crystal growth on the existing nuclei continues until the concentration is reduced to the equilibrium solubility, so that the amount of products is the same as the amount of nucleus and the growth of the bigger particle is faster than that of smaller one. When the growth of $BaTiO_3$ crystal stopped, the growth of $BaTiO_3$ particle is in process by aggregative method. This can be confirmed from our experimental results that the crystal size is constant with that when the reaction time was extended from 48 h to 168 h, but the average particle size increased from 10 nm to 20 nm. At the same time, it is observed that decreasing solution polarity also hinders the particle growth by aggregative method. The $BaTiO_3$ particles prepared using pure water as solvent are made of more crystals than that prepared with mixed solvent, which result in larger particle size. It must be noted that the growth of crystal goes with the growth of particle at elevated temperature. On the other hand, the nucleation mechanism in non-aqueous solvent is possibly not consistent with that in solution containing water. There can be double-nucleation or multi-nucleation existing due to too small amount of water in mixed-solvent reaction system. The increase of total nucleation rate leads to the formation of more crystal seeds and smaller particle size.

4. Conclusions

In this paper, a simple one-pot solvothermal method for the preparation of $BaTiO_3$ ceramic powder with controllable average particle size is described. The particle size of the as-prepared $BaTiO_3$ could easily be tuned by adjusting reaction conditions. With decreasing the water amount in reaction media, the average particle size, the crystal size decrease and the volume of lattice hydroxyl group in $BaTiO_3$ crystal cell increase. Using the non-aqueous solvent, the $BaTiO_3$ powder with average particle size 10 nm and crystal size 8.0 nm can be synthesized at 140°C for 48 h. When the mixed solvent is used as the reaction media, elevated temperature is in favor of formation of tetragonal phase; both elevated temperature and extended time can attain bigger $BaTiO_3$ particle. The results of Raman spectrum show that the as-prepared $BaTiO_3$ powder is tetragonal phase in the local range or cubic phase with some tetragonality. The crystal size of $BaTiO_3$ is mainly dependent on reaction temperature and the ratio of solution. The mechanism of nucleation and growth of

$BaTiO_3$ particle prepared under our experimental condition is followed by dissolution-precipitation mechanism and aggregative method. There could be double-nucleation or multi-nucleation existing due to too small amount of water in the non-aqueous reaction system.

Acknowledgements The financial support from the National Key Nature Science Foundation (No. 20133040) was gratefully acknowledged.

References

1. S. Chatterjee, B.D. Stojanovic, and H.S. Maiti, *Mater. Chem. Phys.*, **78**, 702 (2003).
2. H. Frost, *Key. Eng. Mater.*, **66–67**, 145 (1992).
3. M. Veith, S. Mathur, N. Lecerf, V. Huch, T. Decker, H. Beck, W. Wiser, and R. Haberkorn, *J. Sol-Gel Sci., Technol.*, **15**, 145 (2000).
4. W. Maison, R. Kleeberg, R.B. Heimann, and S. Phanichphant, *J. Euro. Ceram. Soc.,* **23**, 127 (2003).
5. A.V. Prasadarao, M. Suresh, and Sridhar Komarneni, *Mater. Lett.,* **39**, 359 (1999).
6. S. O'Brien, L. Brus, and C.B. Murray, *J. Am. Chem. Soc.*, **123**, 12085 (2001).
7. A. Kareiva, S. Tautkus, R. Rapalaviciute, J.E. Jorgensen, and B. Lundtoft, *J. Mater. Sci.*, **34**, 4853 (1999).
8. J. Moona, E. Suvaci, A. Morrone, S.A. Costantino, and J.H. Adair, *J. Euro. Ceram. Soc.*, **23,** 2153 (2003).
9. H.J. Chen and Y.W. Chen, *Ind. Eng. Chem. Res.*, **42**, 473 (2003).
10. R.M. Piticescu, R.R. Piticescu, D. Taloiand, and V. Badilita, *Nanotechnology*, **14**, 312 (2003).
11. I.J. Clark, T. Takeuchi, N. Ohtoric, and D.C. Sinclaira, *J. Mater. Chem*., **9**, 83 (1999).
12. W.L. Luan and L. Gao, *Ceramics Int.,* **27**, 645 (2001).
13. K.M. Hung, W.D. Yang, and C.C. Huang, *J. Euro. Ceram. Soc.*, **23**, 1901 (2003).
14. S. Wada, T. Tsurumi, H. Chikamori, T. Noma, and T. Suzuki, *J. Crystal Growth*, **229**, 433 (2001).
15. J.F. Bocquet, K. Chhor, and C. Pommier, *Mater. Chem. Phys.*, **57**, 273 (1999).
16. P. Pinceloup, C. Courtois, J. Vicens, A. Lerichea, and B. Thierry, *J. Euro. Ceram. Soc.*, **19**, 973 (1999).
17. B.K. Kim and D.Y. Lim, *J. Amer. Ceram. Soc.*, **86**, 1793 (2003).
18. X.Y. Wang, B.I. Lee, M.Z. Hu, E.A. Payzant, and D.A. Blom, *J. Mater.: Mater. Electronics*, **14,** 495 (2003).
19. Z. Novak, Z. Knez, M. Drofenik, and I. Ban, *J. Non-Crystalline Solids*, **285**, 44 (2001).
20. I.M. Laren and C.B. Ponton, *J. Euro. Ceram. Soc.*, **20**, 1267 (2000).
21. J.Q. Qi, L.T. Li, Y.L. Wang, and Z.L. Gui, *J. Crystal Growth*, **260**, 551 (2004).
22. X.P. Li and W.H. Shih, *J. Amer. Ceram. Soc.*, **80**(11), 2844 (1997).
23. D. Hennings, S. Schreinemacher, *J. Euro. Ceram. Soc.*, **9**, 41 (1992).
24. S. Wada, H. Chikamori, T. Noma, and T. Suzuki, *J. Mater. Sci. Lett.*, **19**, 935 (2000).
25. W.S. Cho, *J. Phys. Chem. Solids*, **l59**, 659 (1998).
26. S. Wada, M. Yano, T. Suzuki, and T. Noma, *J. Mater.Sci.*, **35**, 3889 (2000).
27. S.W. Lu, B.I. Lee, Z.L. Wang, and W.D. Samuels, *J. Crystal Growth*, **219**, 269 (2000).